Network motifs shape distinct functioning of Earth's moisture recycling hubs

Nico Wunderling (nico.wunderling@pik-potsdam.de)
Potsdam Institute for Climate Impact Research https://orcid.org/0000-0002-3566-323X
Frederik Wolf
Potsdam Institute for Climate Impact Research
Obbe Tuinenburg
Utrecht University
Arie Staal
Utrecht University https://orcid.org/0000-0001-5409-1436

Article

Keywords:

Posted Date: March 28th, 2022

DOI: https://doi.org/10.21203/rs.3.rs-1465755/v1

Network motifs shape distinct functioning of Earth's moisture recycling hubs

Nico Wunderling,[1,2,3 *†] Frederik Wolf,[1 *†]
Obbe A. Tuinenburg,[4] Arie Staal[4 *]

[1]Earth System Analysis and Complexity Science, Potsdam Institute for Climate Impact Research (PIK), Member of the Leibniz Association, 14473 Potsdam, Germany
[2]Stockholm Resilience Centre, Stockholm University, Stockholm, SE-10691, Sweden
[3] High Meadows Environmental Institute, Princeton University, Princeton, NJ 08544, USA
[4]Copernicus Institute of Sustainable Development,
Utrecht University, Utrecht, 3584 CB, The Netherlands

[†] These authors contributed equally to this study
*To whom correspondence should be addressed; E-mail: nico.wunderling@pik-potsdam.de, frederik.wolf@pik-potsdam.de, or a.staal@uu.nl.

Earth's hydrological cycle critically depends on the atmospheric moisture flows connecting evaporation to precipitation. Here, we convert a decade of reanalysis-based moisture simulations into a high-resolution global directed network of spatial moisture provisions. We reveal global and local network structures that offer a new view of the global hydrological cycle. We identify four terrestrial moisture recycling hubs: the Amazon Basin, the Congo Rainforest, South Asia and the Indonesian Archipelago. Network motifs reveal contrasting functioning of these regions, where the Amazon strongly relies on directed connections (feed-forward loops) for moisture redistribution and the other hubs on reciprocal moisture connections (zero loops and neighboring loops). Earth's moisture recycling hubs are characterized by specific topologies shaping heterogeneous effects of land-use changes and climatic warming on precipitation patterns.

Life on land relies on the precipitation flows that provide a steady source of freshwater for most areas on Earth. This source enables a resilient Earth System and a safe operating space for humanity[1]. The origins of precipitation over land are almost equally distributed across Earth's land and oceans[2,3]. This implies that not only atmospheric changes such as climate warming, but also modifications at the land surface can affect precipitation patterns on Earth: land-cover transformations including deforestation alter evaporation flows, which may subsequently propagate across continents through evaporation-precipitation cycles[4,5,6]. This process is called atmospheric moisture recycling. Considering how critical they are for the Earth System, we have a surprisingly shallow understanding of how atmospheric moisture flows are arranged.

Recent improvements in atmospheric reanalysis data[7] and methodological advances to track the flows of moisture around the planet at high spatial and temporal resolutions[8] now allow for a significantly more detailed picture of these flows. Previously, we developed a data set of monthly mean atmospheric moisture flows between each pair of 0.5 degree (c. 50 km at the equator) grid cells across the globe[3] (see Methods). One promising approach to analyze these planet-encompassing data is as a spatial network in which each grid cell represents a node that may be connected either uni- or bidirectionally to any other node[9,10,11,12]. A directed link represents a mass flow from source to target, that is, a flow of moisture from its location of evaporation to that of precipitation. Such a network representation can reveal several local and global features of the underlying complex (climate) system[13,14,15]. Specifically, so-called *motifs* are local network structures that control how transitions may cascade across the network and that enable assessing the sensitivity of the network to changes at certain nodes (i.e. grid cells) or edges (i.e. their links)[16,17,18]. Therefore, motifs in the moisture recycling network[4,11,18] may provide novel insights in the structure and functioning of the global hydrological cycle.

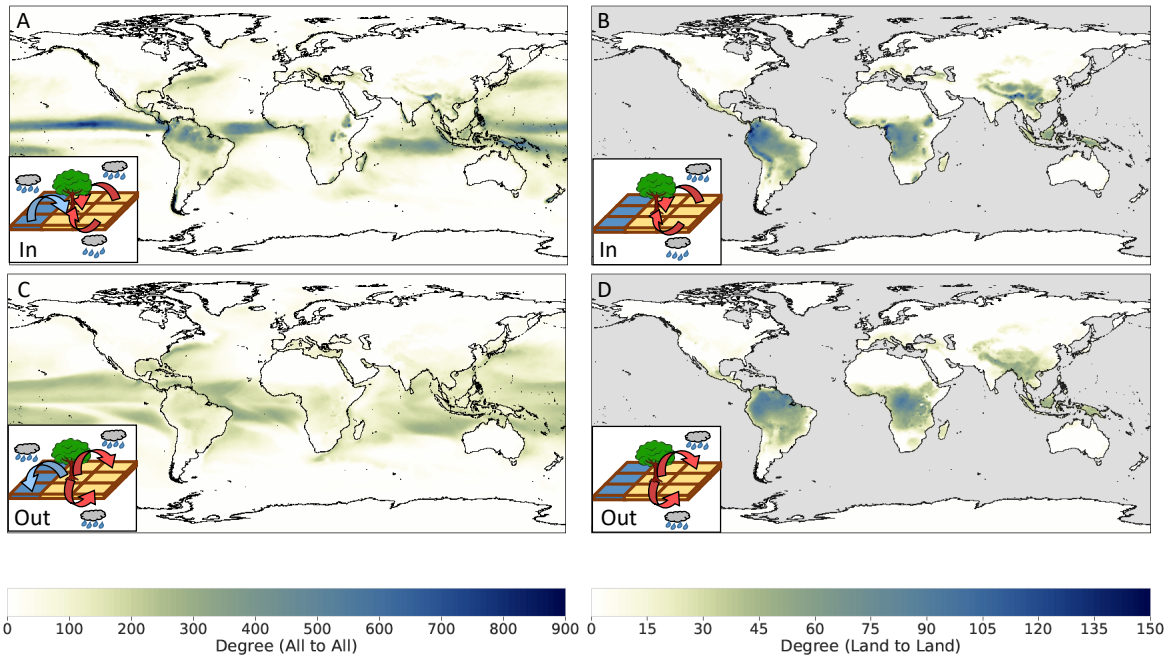

Figure 1 | In- and out-degree of the global moisture recycling network. A,C, In- and out-degree for all connections, and **B,D,** solely for land to land interactions. High in-degree refers to nodes/grid cells receiving moisture from many other grid cells. Elevated out-degree refers to moisture distributors. Insets illustrate the depicted measures.

Results

Hubs in the global moisture recycling network. Here, we apply a network approach to high-resolution global atmospheric moisture flows. We build a directed, unweighted network[19,9,20] featuring the strongest links carrying $\rho = 25\%$ of the global moisture flow based on the global atmospheric simulations[8]. Although $\rho = 25\%$ is a choice we made based on the moisture flow strength distribution (see Fig. S1), our results are robust to substantial changes of ρ (see sensitivity analyses in the Methods). As an initial step, we study the in-degree and out-degree of the moisture recycling network[21] (Fig. 1A,C), indicating the number of incoming and outgoing connections of each node. The tropics stand out as the region with the most intense moisture transport regarding both in- and out-degree. However, the pattern of out-degree differs systematically from that of in-degree, without marked regions that have outstanding out-degree maxima. Indeed, the stronger cutoff in the out-degree distributions (Figs. S10, S11) demonstrates a first significant finding: in-degree is consistently broader distributed than out-degree, indicating the existence of super-receivers but the absence of super-distributors of moisture. We study the dependency of regions on recycling-based moisture influx by considering particular link classes. Of particular interest are moisture flows from land to land (Fig. 1B,D), as these not only serve as main water supply to many regions but are also directly modulated by human activities that alter the land surface moisture fluxes, such as deforestation and irrigation[22]. Globally, we identify four main hubs of large in- and out-degree in the land to land network (Fig. 1B,D): the Amazon Basin (AB), Congo Rainforest (CR), Indonesian Archipelago (IA) and South Asia (SA). A deeper analysis of the topology of the network reveals the fundamentally differing functioning of the four regions.

Motifs shape ecosystem functioning. Specifically, we identify feed-forward loops (FFL), zero loops (ZL) and neighboring loops (NBr, see explanatory insets in Fig. 2). FFLs involve three

nodes linked in a directed triangular way, creating a lensing effect of moisture flow. This means that moisture flows from source to target are larger than they appear from analyzing direct flows only. ZLs consist of two nodes with a bidirectional, reciprocal connection. In other words, they show the feedback between two nodes in the network, such that hydrological change in one node gets amplified through its interaction with the other. NBrs indicate directed reciprocity: they describe a zero loop connected to an additional source node that induces a directed moisture flow towards the ZL. Like FFLs, they involve three nodes and have a flavor of directedness in their topology. Thus, they share features of both node-to-node dependency and a lensing effect. NBrs imply that land-cover or atmospheric change in the source node could disrupt the hydrological feedback between two other nodes. In line with their functionality, we refer to spatial conglomerates of FFLs as *directed lenses*, to those of NBr as *directed corridors*, and to regions with an overwhelming fraction of ZLs as *washing machines* due to the circular nature of moisture flow. Perturbations in directed lenses of corridors may propagate in a spatially predictable (directed) manner, whereas in case of washing machines they may spread in an unpredictable or perhaps spatially uniform way.

We find that edges and nodes are highly involved and locally organized in motifs: in the all to all network (land to land network) each edge is on average part of $\sim$100 ($\sim$40) motifs and each node is involved in $\sim$5000 ($\sim$250) motifs. This implies that the network as a whole is highly locally organized by motifs, and indeed, motifs appear approximately two orders of magnitude more often than we would expect from a random graph (see supplementary results in SI and Figs. S13, S14). Going beyond classical degree measures, we compare the presence of FFLs and ZLs, and that of FFLs and NBrs (Fig. 2), both across the globe and for land flows only. Specifically, we study the per-node motif strength as relative values rescaled to their respective global maximum per-node count (for details, see Methods).

ZLs are ubiquitous across large parts of the planet (Fig. 2A-D), signifying widespread reciprocity in moisture flows. An oceanic exception can be found in the Pacific, where we observe how the Hadley cycle is represented in the network: rising air over the equator, falling air over the subtropics, and a surface return flow towards the equator results in many ZLs over the subtropics but dominating FFLs over the surface return flow areas (Fig. 2A).

Upon replacing ZLs by NBrs in the all to all network (Fig. 2E, cf. Fig. 2A), the FFLs become more important. This is a direct consequence of a large normalized number of ZLs in the overall network that are not connected to a third node. However, selecting the land to land connections only (Fig. 2F) leads to a considerable shift in the dominant network motif, as much fewer FFLs are present. This underlines that much of the land to land directedness in the global moisture recycling network is carried by NBrs and, thus, via moisture corridors. In contrast, much of the ocean-to-land connectivity is organized through FFLs via moisture lensing.

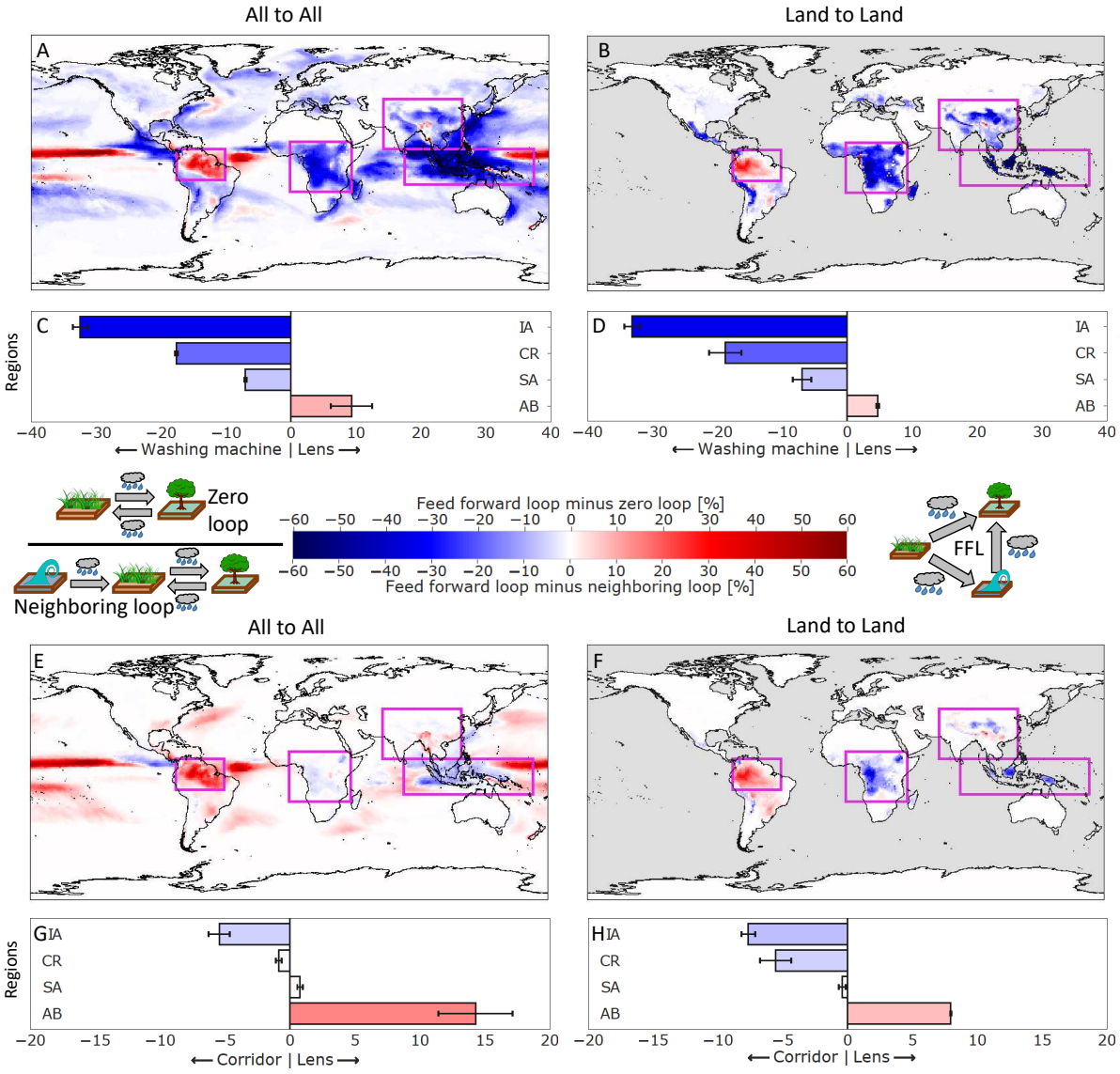
All to All
Land to Land
A
B
C
D
Regions
IA
CR
SA
AB
−40 −30 −20 −10 0 10 20 30 40
⟵ Washing machine | Lens ⟶
Zero loop
Neighboring loop
Feed forward loop minus zero loop [%]
−60 −50 −40 −30 −20 −10 0 10 20 30 40 50 60
Feed forward loop minus neighboring loop [%]
FFL
All to All
Land to Land
E
F
G
H
−20 −15 −10 −5 0 5 10 15 20
⟵ Corridor | Lens ⟶

Figure 2 | Characterization of the Earth's moisture recycling hubs. A, FFL and ZL strength difference for the all to all network and **B,** for the land to land network. The corresponding spatially aggregated averages are shown in panels **C** and **D**. Illustrations next to the colorbar schematically illustrate the motifs. The four main moisture recycling regions can be clearly distinguished. More red colors represent larger lensing of moisture flows; more blue colors represent reciprocity of the network structure (AB is a directed lens, while IA, CR and SA are washing machines in descending order). **E-H,** Same as **A-D** but for FFL and NBr. More red colors represent larger lensing effects and more blue colors indicate directed corridors (AB is a directed lens, IA is a directed corridor). The differences between the all to all network and the land to land network (mainly regarding the AB and the CR) highlight the differences between the ocean to land connectivity (which is included in the all to all network) and the organization of moisture recycling over land. The error bars are are derived from a sensitivity analysis in which we analyze the moisture recycling network for a variable network threshold ρ in the range from 20%, to 30% (see SI Figs. S5-S8).

Motif strength characterizes network hubs. When we compare the spatially aggregated average motif strength difference per focus region, an interesting difference emerges (Figs. 2C-D, 2G-H). From both, the all to all and the land to land network arises the same pattern: the Amazon is a *directed lens* whereas especially in the Indonesian Archipelago and the Congo the less directed motifs dominate. For the Amazon, it is known that effects of forest loss are propagated downwind, mainly westward from the Atlantic Ocean towards the Andes and southward out of the basin[4,5]. Our results reveal that the strong directedness of moisture propagation in the Amazon is globally one-of-a-kind, pointing at a unique role of Earth's largest rainforest in its regional hydrological cycle, and its particular vulnerability. The cause of this exceptional functioning is unclear. Possibly, it reflects the "biotic pump hypothesis," which states that the large-scale condensation of water vapor creates horizontal pressure differences in the lower atmosphere that propel local atmospheric dynamics[23]. Regardless of the mechanism, locations at the receiving end of a FFL will be particularly sensitive to deforestation at the

source of the motif.

The other major tropical rainforests are characterized by reciprocal effects, indicated mainly by the ubiquity of ZLs. This suggests that these regions may exhibit a more local and diverse response to land-use change or shifts in the moisture distribution. Positive as well as negative changes in a certain location would affect that location not only directly but also indirectly. This may knock ecosystems more easily out of equilibrium, as loss of evaporation will cause a local loss in precipitation as well. However, it could also support regrowth and reforestation of degraded or disturbed forests, as the resulting recovery of evaporation would recover precipitation locally as well. Put otherwise, the "hidden" local forest-precipitation feedback due to ZLs expands the local-scale hysteresis of tropical tree cover against precipitation levels that is believed to be widespread across the tropics[24].

Outside the tropics, South Asia is a hotspot of ZLs. This may be related to the Himalaya, given that other mountain regions across the globe have relatively many ZLs as well (Fig. 2). This could be due to a relatively localized hydrological cycle or seasonality in the direction of moisture flow. Indeed, also other regions that are not identified as hubs from a degree perspective have relatively many ZLs, namely monsoon (e.g. West Africa and North America) and mountainous regions (e.g. the Alps and Caucasus), which are characterized by seasonal, high intensity moisture flows from ocean to land. These could relatively easily generate strong reciprocal dependencies at annual time scales.

Discussion

Our network approach reveals features of the global hydrological cycle that have been overlooked in previous analyses. Considering that particularly FFLs have been proven to increase

the possibility of cascading tipping in networks of tipping elements[18], we here present an additional argument for assessing the robustness of Earth's major moisture recycling hubs. It is feared that the Amazon rainforest may tip as a result of deforestation and climate change[25]. Weakening of links from the network may heavily affect moisture flows down the network. Such cascading effects may additionally be amplified by climate change: the propagation of droughts through a network dominated by FFLs expands the area hit by such events and could possibly increase the chances of exceeding thresholds for tipping cascades[18]. Furthermore, as the atmosphere warms, it can contain more water vapor. On a global scale, this increase is predicted to be larger than the concurrent increases in evaporation and precipitation, meaning that atmospheric moisture recycling will tend to occur over larger distances[26], altering the topology of Earth's moisture recycling network.

In contrast to the overwhelming majority of studies employing climate networks where the connections in the network are based upon a statistical similarity of measured time series[13,27,28,29,30,31], our network represents directed causal connections. This, first, allows for a straightforward interpretation of the measured results and, second, opens up many pathways for subsequent research: analyzing higher-order network measures, such as betweenness[20,28,32], could identify connectors in the network; investigating the temporal evolution of the moisture recycling network, such as for the impact of different phases of the El Niño Southern Oscillation[33], could help explain climatic anomalies; and developing networks using climate-change projections could offer a new view on Earth System functioning under global warming.

Methods

UTrack atmospheric moisture tracking model. The UTrack atmospheric moisture tracking model is a novel Lagrangian model that tracks parcels of moisture forward in three-dimensional space[8]. UTrack is the first moisture tracking model to employ ERA5 reanalysis data[7]. The basic principle of the model is that for each mm of evaporation, a certain number of "moisture parcels" is released and subsequently tracked through time and space. At each time step, the moisture budget of the parcels is updated based on evaporation and precipitation at the respective time and location, meaning that for each location of evaporation, a detailed image of the "footprint" of evaporation can be created. All types of evapotranspiration are included, and here simply called evaporation.

For each mm of evaporation, 100 parcels are released 50hPa above the surface height at random spatial locations within each 0.25 degree grid cell of input evaporation data. The trajectories of the parcels are based on interpolated three-dimensional ERA5 wind speed and wind direction data, which also have a horizontal resolution of 0.25 degrees and consist of 25 pressure layers in the atmospheric column. The spatial coordinates of each parcel are updated at each time step of 0.1 hours. Also at each time step, there is a certain probability that a parcel is redistributed randomly along the atmospheric column such that, on average, every parcel is redistributed every 24 hours (see methods section *Moisture recycling data set: validation and uncertainties* below for further details). The relative probability of the new position in the atmospheric column is scaled with the vertical moisture profile. Parcels are tracked for 30 days or until 99% of their moisture has precipitated.

To allocate a certain fraction of any moisture parcel to precipitation events at the current time and location, ERA5 hourly total precipitation (P) and total precipitable water (TPW) are interpolated to the simulation time step of 0.1 hours. The amount of moisture that precipitates at a certain time step equals the amount of precipitation at that time step over the total precipitable

water in the atmospheric water column (P/TPW). Specifically, precipitation A in mm per time step at location x, y at time t that originated as evaporation from a particular source is described as:

$$A_{x,y,t} = P_{x,y,t} \frac{W_{\text{parcel,t}} E_{\text{source,t}}}{TPW_{x,y,t}} \tag{1}$$

with P being precipitation in mm at time step t, $W_{\text{parcel,t}}$ (mm) the amount of moisture in the parcel of interest, $E_{\text{source,t}}$ the fraction of moisture present in the parcel at time t that has evaporated from the source, and TPW (mm) the precipitable water in the atmospheric water column. The moisture content of parcels is updated each time step using evaporation and precipitation at its current location:

$$W_{\text{parcel,t}} = W_{\text{parcel,t-1}} + (E_{\text{x,y,t}} - P_{\text{x,y,t}}) \frac{W_{\text{parcel,t-1}}}{TPW_{\text{x,y,t}}} \tag{2}$$

The moisture (fraction) that has evaporated from the source is updated as follows:

$$E_{\text{source,t}} = \frac{E_{\text{source,t-1}} W_{\text{parcel,t-1}} A_{x,y,t}}{W_{\text{parcel,t}}} \tag{3}$$

The moisture flow m_{ij} from evaporation in cell i to precipitation in cell j is aggregated on a monthly basis (mm/month), where $[x, y] \in j$ becomes:

$$m_{ij} = \sum_{t=0}^{\text{month}} A_{j,t} \frac{E_{i,t}}{W_{i,t}} \tag{4}$$

with $W_{i,t}$ being the tracked amount of moisture from the source cell i at time t. These simulations were performed for all evaporation on Earth during 2008–2017. The results were then aggregated on a mean-monthly basis to produce monthly climatologies, and stored at 0.5

degree resolution. This data set can be downloaded from[34]. For details on how to process the data, we refer to the accompanying paper by Tuinenburg et al. (2020)[3].

Moisture recycling data set: validation and uncertainties. As with all moisture recycling simulations, the ones used in this study rely on a number of assumptions that may affect the moisture recycling rates. All off-line moisture recycling models use atmospheric model output to simulate the path of evaporation through the atmosphere to the location where it precipitates. Therefore, there are two sources of uncertainty that affect the moisture recycling estimates: 1. the quality of the atmospheric forcing data and 2. the assumptions in the moisture tracking model.

Tuinenburg and Staal (2020)[8] explored these sources of uncertainty for a number of locations globally. The effects of a decrease in quality of the atmospheric forcing data was most important in the vertical resolution of the atmospheric data: the forcing data should have enough vertical levels to resolve any vertical shear in atmospheric moisture transport. If the forcing data has a low vertical resolution, the moisture tracking model is forced with the mean atmospheric flow over a number of layers. In many regions, there are surface moisture flows that are in a different direction than the moisture flow aloft, resulting in a very small vertically integrated transport, which would distort the simulation of the atmospheric moisture transport. Compared to the vertical resolution of the forcing data, the horizontal and temporal resolutions where less important. Because of the importance of this high vertical resolution, it was recommended[8] to use the ERA5 data set[7] as its forcing data set, as this currently is the atmospheric reanalysis data set with the highest vertical resolution.

The uncertainties due to the assumptions in the moisture tracking model can be split in a category of simulation assumptions and physical assumptions. The simulation assumptions include model formulation (Eulerian vs. Lagrangian model set-ups), time step lengths, number of

parcels released and types of interpolation. Of these simulation assumptions, the most important aspects were the model formulation, with Lagrangian models better able to resolve complex terrain and atmospheric flows. For the other model assumptions (see methods section *UTrack atmospheric moisture tracking model*), it was chosen to simulate with the highest level of precision before any more information (e.g. more parcels) would no longer affect evaporation footprints and moisture recycling statistics (see[8] for further details).

The results of UTrack have recently been validated across the tropics by independent measurements of deuterium excess, a measure of a stable isotope that depends on terrestrial precipitation recycling[35]. UTrack estimates and isotope-based estimates of terrestrial moisture recycling corresponded, especially in tropical rainforests (Kendall's $\overline{\tau} = 0.52$[35]), which are found to be moisture recycling hubs on a global scale.

Network construction. Motivated by the network-like structure of the data, we here employ a network perspective to study moisture flows. Hence, nodes in such a network are grid cells on a regular spherical grid and edges represent the moisture transported. However, interpreting the data set directly as a weighted network is neither computationally feasible nor does a weighted network allow for identifying motifs, the building blocks of complex networks. We, therefore, aim for an approach utilizing an unweighted network.

As shown in Fig. S1, moisture recycling strengths are heterogeneously distributed over multiple powers of magnitude. Thus, it is not appropriate to just withdraw the moisture transport volume and include all moisture transport connections within the data set as equal and unweighted links. Instead, we attempt to highlight the strongest moisture pathways and thus the backbone of the Earth's moisture recycling network. To on the one hand include as much moisture volume as possible but also keep the absolute volume of moisture transport represented per edge as similar as possible, we decided to include edges in a data-adaptive way: we step-wise

include links starting from the strongest and stop this procedure as the total moisture transport volume exceeds the variable threshold ρ. The resulting edges then represent the backbone of the global moisture recycling network. In the main text, we have shown the results for a network where all edges together represent $\rho = 25\%$ of the total moisture transport. Here and in the SI figures, we add a sensitivity analysis for $\rho = 20\%$ and $\rho = 30\%$ and find that the results are stable for this broader range of total moisture volume thresholds.

Network measures and motifs. The topology of an unweighted network is typically encoded in an adjacency matrix $\mathbf{A}$ with elements a_{ij} indicating if there exists an edge from node i to node j (a_{ij}=1) or not (a_{ij}=0). The degree k of a node i describes the number of adjacent edges pointing towards or away from a node i. Hence, the in-degree is defined by[21]

$$k_{in}^{i} = \sum_{i=1}^{N} a_{ji} \tag{5}$$

and out-degree is defined by[21]

$$k_{out}^{i} = \sum_{i=1}^{N} a_{ij}. \tag{6}$$

To further analyze the topology of a network and, in particular, the local connectivity patterns, we study the presence of three motifs – the feed forward loop, the neighboring loop and the zero loop.

The feed forward loop (FFL) consists of three nodes A,B,C where nodes A and C are directly connected and via a detour over node B (intermediary node). Therefore, we have two different pathways that focus on node C. Hence, this motif can be referred to as a directed lens, due to its focused flow from two nodes on one singular and its purely directed linkage. This network motif has been studied in the context of tipping elements and has been proven to facilitate tipping cascades by lowering critical thresholds[18]. The zero loop (ZL) is made up by a bidirectional connection of two nodes. In contrast to the FFL where node A does not receive feedback from

node C, here both nodes are dependent on each other without a preferred direction of network flow. This facilitates tipping to a much lesser degree than the FFL motif[18]. The neighboring loop (NBr) is an extension of the ZL. In this case, there is an additional node connected to one of the nodes of a zero loop. Hence, there is a two-step directionality in the motif, but in contrast to the FFL, this motif is characterized by reciprocity.

We count the number of motifs a certain node is involved in the network. Doing this, each node is characterized by its number of FFLs, ZLs and NBrs.

Motif strength and spatially aggregated motif strength difference. To assess the presence of motifs and, in particular, their relative frequency, we first determine the numbers of FFLs, ZLs and NBrs per node. Subsequently, we normalize these counts by the respective maximum to obtain the motif strength which is shown for each network motif in Fig. S2. In Fig. S2A,B,C, we display the motifs for the global network and in Fig. S2D,E,F for the land to land network. To specifically characterize the focus regions by means of the network topology, we evaluate which motifs dominate in which region. Consequently, we compute the difference of the motif strengths shown in Fig. S2 and reveal the patterns shown in Fig. 2. For spatially aggregated motif strength differences (Fig. 2C,D), we then compute the average of the respective values inside the highlighted boxes.

Sensitivity to link threshold ρ. The network analysis featured in the main text uses those moisture recycling edges that together represent $\rho = 25\%$ of all atmospheric moisture recycling on Earth. The aim of this thresholding procedure is to utilize a network approach with unweighted edges but also taking into account the large spread of moisture recycling strengths. To test the robustness of the results to the threshold value, we here show the same figures as above in the main text but with different thresholds ρ. Note that the error bars in Fig. 2 are based on

the analysis featured in this part (the resulting differences using thresholds of $\rho = 20\%$ and $\rho = 30\%$).

Figs. S3 and S4 show the in- and out-degree of the all to all and land to land network using a threshold of $\rho = 20\%$ (Fig. S3) and $\rho = 30\%$ (Fig. S4). Note that the colorbar has been adjusted as the number of links differs substantially between the networks. The main difference between Fig. S3 and Fig. S4 is the greater emphasis of moisture recycling in the mid-latitudes in Fig. S4. This is a direct consequence of considering more, and thus also some weaker, links. Acknowledging this difference, we stress that especially the land to land patterns (Fig. S3C,D and Fig. S4C,D) are consistent. In particular, the four focus regions as defined in the main text stand out as the main global land to land moisture recycling hubs. To support this visual analysis of the in- and out-degree pattern, we furthermore compute the motif strengths for both network configurations for a quantitative validation of the results.

In line with the main text, we compare the FFL and ZL strength (see Fig. 2A-D). Not only the spatial patterns in our sensitivity analysis agrees remarkably well with the results in the main text above, but also the focus regions remain basically the same (compare Fig. S5 for $\rho = 20\%$ and Fig. S6 for $\rho = 30\%$ with Fig. 2). The only slight change is the shift towards a directed lens (spatially aggregated FFL and ZL strength difference) for the Amazon basin in the all to all network for increasing ρ (compare Fig. S5C vs Fig. S6C vs Fig. 2C). We attribute the overproportional increase of the number of FFLs to those that include at least one oceanic grid cell to this noticeable shift. This underscores our characterization of the Amazon basin as a directed lens.

The spatially aggregated FFL and NBr difference (Figs. S7 and S8) is structurally the same as above, where we computed the FFL and ZL difference (see Fig. S5 and S6). The spatial patterns and the aggregated values are robust against shifts of ρ. However, for the Amazon basin (AB), the number of FFLs increases overproportionally in the all to all network when we

include more links into our analysis. In other words, the spatially aggregated FFL-strength for AB increases for higher thresholds ρ (compare Figs. S7C, S8C and Fig. 2G).

Sensitivity to the size of the focus regions. Another aspect affecting the results is the spatial extent chosen as a focus region (i.e. the rectangles in Fig. 2). Varying the size of these rectangles affects the spatially aggregated measures. For all focus regions beside the Amazon Basin (AB), the values are not significantly affected by changing the rectangle size, as the values close to the focus regions are either coherently negative, as for the Congo Rainforest (CR) and the Indonesian Archipelago (IA), or close to zero (South Asia: SA). The AB is characterized by positive values (tendency to lensing) whereas the more southern parts along the Andes are marked by more negative (corridor/washing machine) values.

Hence, we assess the stability of the results by using the spatial region covered by the Amazon rainforest (extent of the Amazon rainforest is based on[5]) and compare them to the ones obtained by using the rectangle. The results featured in Fig. S9 indicate that only considering the rainforest covered parts of the AB leads to similar or even more positive (lensing) values, confirming our conclusions that the Amazon rainforest region functions differently from the other focus regions.

Notes on colour maps. This paper makes use of perceptually uniform colour maps developed by F. Crameri[36].

Data and Code availability. The data and code that support the findings of this study are available from the corresponding authors upon request.

References and Notes

[1] Wang-Erlandsson, L. *et al.* Towards a green water planetary boundary. *Nature Reviews Earth & Environment* **accepted** (2022).

[2] van der Ent, R. J., Savenije, H. H. G., Schaefli, B. & Steele-Dunne, S. C. Origin and fate of atmospheric moisture over continents. *Water Resources Research* **46** (2010). URL https://agupubs.onlinelibrary.wiley.com/doi/abs/10.1029/2010WR009127. https://agupubs.onlinelibrary.wiley.com/doi/pdf/10.1029/2010WR009127.

[3] Tuinenburg, O. A., Theeuwen, J. J. E. & Staal, A. High-resolution global atmospheric moisture connections from evaporation to precipitation. *Earth System Science Data* **12**, 3177–3188 (2020). URL https://essd.copernicus.org/articles/12/3177/2020/.

[4] Zemp, D. C. *et al.* On the importance of cascading moisture recycling in South America. *Atmospheric Chemistry and Physics* **14**, 13337–13359 (2014).

[5] Staal, A. *et al.* Forest-rainfall cascades buffer against drought across the Amazon. *Nature Climate Change* **8**, 539–543 (2018).

[6] O'Connor, J. C. *et al.* Forests buffer against variations in precipitation. *Global Change Biology* **27**, 4686–4696 (2021). URL https://onlinelibrary.wiley.com/doi/abs/10.1111/gcb.15763. https://onlinelibrary.wiley.com/doi/pdf/10.1111/gcb.15763.

[7] Hersbach, H. *et al.* The era5 global reanalysis. *Quarterly Journal of the Royal Meteorological Society* **146**, 1999–2049 (2020). URL https://rmets.

onlinelibrary.wiley.com/doi/abs/10.1002/qj.3803. https://rmets.onlinelibrary.wiley.com/doi/pdf/10.1002/qj.3803.

[8] Tuinenburg, O. A. & Staal, A. Tracking the global flows of atmospheric moisture and associated uncertainties. *Hydrology and Earth System Sciences* **24**, 2419–2435 (2020). URL https://hess.copernicus.org/articles/24/2419/2020/.

[9] Newman, M. E. The structure and function of complex networks. *SIAM Review* **45**, 167–256 (2003).

[10] Donges, J. F., Zou, Y., Marwan, N. & Kurths, J. Complex networks in climate dynamics. *Eur. Phys. J. Spec. Top.* **174**, 157–179 (2009).

[11] Zemp, D. C., Wiedermann, M., Kurths, J., Rammig, A. & Donges, J. F. Node-weighted measures for complex networks with directed and weighted edges for studying continental moisture recycling. *EPL (Europhysics Letters)* **107**, 58005 (2014).

[12] Krönke, J. *et al.* Dynamics of tipping cascades on complex networks. *Physical Review E* **101**, 042311 (2020).

[13] Boers, N. *et al.* The South American rainfall dipole: A complex network analysis of extreme events. *Geophys. Res. Lett.* **41**, 7397–7405 (2014).

[14] Molkenthin, N. *et al.* Edge anisotropy and the geometric perspective on flow networks. *Chaos* **27**, 035802 (2017).

[15] Wolf, F., Kirsch, C. & Donner, R. V. Edge directionality properties in complex spherical networks. *Phys. Rev. E* **99**, 012301 (2019).

[16] Milo, R. *et al.* Network motifs: simple building blocks of complex networks. *Science* **298**, 824–827 (2002).

[17] Alon, U. Network motifs: theory and experimental approaches. *Nature Reviews Genetics* **8**, 450–461 (2007).

[18] Wunderling, N. *et al.* How motifs condition critical thresholds for tipping cascades in complex networks: Linking micro-to macro-scales. *Chaos: An Interdisciplinary Journal of Nonlinear Science* **30**, 043129 (2020).

[19] Albert, R. & Barabási, A.-L. Statistical mechanics of complex networks. *Rev. Mod. Phys.* **74**, 47 (2002).

[20] Molkenthin, N., Rehfeld, K., Marwan, N. & Kurths, J. Networks from Flows - From Dynamics to Topology. *Sci. Rep.* **4**, 1–5 (2014).

[21] Barabási, A.-L. & Pósfai, M. *Network Science* (Cambridge University Press, 2016).

[22] Keys, P. W., Wang-Erlandsson, L. & Gordon, L. J. Revealing invisible water: Moisture recycling as an ecosystem service. *PLOS ONE* **11**, 1–16 (2016). URL `https://doi.org/10.1371/journal.pone.0151993`.

[23] Makarieva, A. M. & Gorshkov, V. G. Biotic pump of atmospheric moisture as driver of the hydrological cycle on land. *Hydrology and Earth System Sciences* **11**, 1013–1033 (2007). URL `https://hess.copernicus.org/articles/11/1013/2007/`.

[24] Hirota, M., Holmgren, M., Van Nes, E. H. & Scheffer, M. Global resilience of tropical forest and savanna to critical transitions. *Science* **334**, 232–235 (2011).

[25] Lovejoy, T. E. & Nobre, C. Amazon tipping point: Last chance for action. *Science Advances* **5**, eaba2949 (2019).

[26] Gimeno, L. *et al.* The residence time of water vapour in the atmosphere. *Nature Reviews Earth & Environment* **2**, 558–569 (2021).

[27] Tsonis, A. A. & Roebber, P. J. The architecture of the climate network. *Phys. A* **333**, 497–504 (2004).

[28] Donges, J. F., Zou, Y., Marwan, N. & Kurths, J. The backbone of the climate network. *EPL* **87**, 48007 (2009).

[29] Boers, N. *et al.* Complex networks reveal global pattern of extreme-rainfall teleconnections. *Nature* **566**, 373–377 (2019).

[30] Wolf, F., Bauer, J., Boers, N. & Donner, R. V. Event synchrony measures for functional climate network analysis: A case study on South American rainfall dynamics. *Chaos* **30**, 033102 (2020).

[31] Ludescher, J. *et al.* Network-based forecasting of climate phenomena. *Proceedings of the National Academy of Sciences* **118** (2021).

[32] Newman, M. E. J. A measure of betweenness centrality based on random walks 1–15 (2003). URL http://arxiv.org/abs/cond-mat/0309045. 0309045.

[33] Sorí, R., Nieto, R., Liberato, M. L. R. & Gimeno, L. Oceanic versus terrestrial origin of el niño southern oscillation–associated continental precipitation anomalies. *Annals of the New York Academy of Sciences* **1504**, 202–214 (2021). URL https://nyaspubs.onlinelibrary.wiley.com/doi/abs/10.1111/nyas.14665. https://nyaspubs.onlinelibrary.wiley.com/doi/pdf/10.1111/nyas.14665.

[34] Tuinenburg, O. A., Theeuwen, J. J. E. & Staal, A. Global evaporation to precipitation flows obtained with Lagrangian atmospheric moisture tracking (2020). URL https://doi.org/10.1594/PANGAEA.912710. PANGAEA, doi: 10.1594/PANGAEA.912710.

[35] Cropper, S. *et al.* Comparing deuterium excess to large-scale precipitation recycling models in the tropics. *npj Climate and Atmospheric Science* **4**, 60 (2021).

[36] Crameri, F. Geodynamic diagnostics, scientific visualisation and staglab 3.0. *Geoscientific Model Development* **11**, 2541–2562 (2018).

Acknowledgements

N.W. acknowledges support from the European Research Council Advanced Grant project ERA (Earth Resilience in the Anthropocene, ERC-2016-ADG-743080). F.W. is grateful for financial support by the BMBF grant climXtreme (No. 01LP1902J) "Spatial synchronization patterns of heavy precipitation events". The authors gratefully acknowledge the European Regional Development Fund (ERDF), the German Federal Ministry of Education and Research and the Land Brandenburg for supporting this project by providing resources on the high performance computer system at the Potsdam Institute for Climate Impact Research.

Author contributions

N.W. and F.W. contributed equally to this study. N.W. conceived the study. All authors have designed the study. N.W. and F.W. conducted the network analysis and the simulation runs. F.W. led the writing of the manuscript with input from all authors. N.W. designed the figures with input from all authors. A.S. and O.A.T. developed the atmospheric moisture recycling dataset. A.S. supervised this study.

Additional information

Supplementary information is available in the online version of the paper. Reprints and permissions information are available online at www.nature.com/reprints. Requests for materials should be addressed to N.W. and F.W.

Competing interests

The authors declare no competing interests.

Supplementary Files

This is a list of supplementary files associated with this preprint. Click to download.

- supplement.pdf